

---

# Efficient Black-Box Adversarial Attack Guided by the Distribution of Adversarial Perturbations

---

Yan Feng<sup>1</sup>, Baoyuan Wu<sup>2</sup>, Yanbo Fan<sup>2</sup>, Zhifeng Li<sup>2</sup>, Shutao Xia<sup>1</sup>

<sup>1</sup>Tsinghua Shenzhen International Graduate School, Tsinghua University, China

<sup>2</sup>Tencent AI Lab, China

wubaoyuan1987@gmail.com; xiast@sz.tsinghua.edu.cn

## Abstract

This work studied the score-based black-box adversarial attack problem, where only a continuous score is returned for each query, while the structure and parameters of the attacked model are unknown. A promising approach to solve this problem is evolution strategies (ES), which introduces a search distribution to sample perturbations that are likely to be adversarial. Gaussian distribution is widely adopted as the search distribution in the standard ES algorithm. However, it may not be flexible enough to capture the diverse distributions of adversarial perturbations around different benign examples. In this work, we propose to transform the Gaussian-distributed variable to another space through a conditional flow-based model, to enhance the capability and flexibility of capturing the intrinsic distribution of adversarial perturbations conditioned on the benign example. Besides, to further enhance the query efficiency, we propose to pre-train the conditional flow model based on some white-box surrogate models, utilizing the transferability of adversarial perturbations across different models, which has been widely observed in the literature of adversarial examples. Consequently, the proposed method could take advantages of both query-based and transfer-based attack methods, to achieve satisfied attack performance on both effectiveness and efficiency. Extensive experiments of attacking four target models on CIFAR-10 and Tiny-ImageNet verify the superior performance of the proposed method to state-of-the-art methods.

## 1 Introduction

It has been well known [2, 13] that adversarial examples are the serious threat to deep neural networks. Although massive attack methods have been developed, most of them assume that all information of the attacked model is accessible, such that the gradient can be easily computed to generate adversarial perturbations, which is called *white-box* adversarial attack. However, a more practical setting in real world scenarios is that the structure and parameters of the attacked model is inaccessible to the attacker, while only the feedback of each query is provided, which is called *black-box* adversarial attack. Further, if the feedback is only the discrete label, then it is dubbed *decision-based* black-box attack; if the feedback is the continuous score (*e.g.*, the posterior probability w.r.t. each class), then it is dubbed *score-based* black-box attack, which is also the focus of this work.

The score-based black-box attack can be formulated as a derivative-free optimization problem. A promising derivative-free optimization approach is evolution strategies (ES) [38]. The core idea of the ES-based black-box attack is introducing a search distribution to model the distribution of adversarial perturbations. Given the search distribution, several perturbations are sampled to obtain new queries to the attacked model; then, the query feedbacks are adopted to update the search distribution to get better values of the black-box objective function. The Gaussian distribution is widely used as the search distribution in many ES methods [44, 40, 17]. However, we don't think

\*This work was done when Yan Feng was an intern at Tencent AI Lab. Correspondence to: Baoyuan Wu and Shutao Xia.

that the simple Gaussian distribution is a good choice for modeling the distribution of adversarial perturbations. Because it ignores the close dependency between adversarial examples and benign examples. Considering that even the loss landscapes around different benign examples are quite diverse, it is difficult to imagine that the adversarial perturbations around different benign examples could follow one identical distribution. A recent work in ES [12] proposed to transform the Gaussian-distributed variable to another space through a reversible flow-based generative model, such that the modeling capability for probabilistic distributions is enhanced. However, the flow-based model doesn't take into account the variation due to benign examples. Inspired by that work, we propose to adopt a conditional generative flow model, called *c-Glow*, which is expected to be flexible enough to capture the complex distribution of adversarial perturbations conditioned on diverse benign examples.

However, due to the additional parameters of *c-Glow*, it may require more queries to learn a good approximation of the distribution of adversarial perturbations, while the query is the main cost in the black-box attack. To accelerate the attack efficiency, we propose to pre-train the *c-Glow* model based on some white-box surrogate models, according to the observation [33, 34, 28] that adversarial examples generated for one model may also be adversarial for another model, dubbed *adversarial transferability*. Specifically, we propose to minimize the K-L divergence between the *c-Glow* model and the energy-based model w.r.t. the adversarial loss, based on surrogate models. Consequently, the proposed method utilizes the advantages from both query-based and transfer-based attack methods, with the expectation to achieve high adversarial success rate and high attack efficiency simultaneously.

The main contributions of this work are three-fold. **1)** We propose to utilize the conditional Glow model coupled with Gaussian as the search distribution in the ES algorithm for solving the score-based black-box adversarial attack problem. **2)** We propose to pre-train the *c-Glow* model via approximating the energy-based model of the perturbation distribution of surrogate models. **3)** Extensive experiments on benchmark datasets demonstrate the superiority of the proposed attack method to several state-of-the-art methods.

## 2 Related Work

Here we only focus on black-box adversarial attack methods, which can be generally partitioned to two categories, including *decision-based* and *score-based* adversarial attacks.

**Decision-based Adversarial Attacks.** For decision-based attacks, an attacker can only acquire the output label of the target model. A boundary search method [3] randomly sampled candidate perturbations following the normal distribution, and the perturbation with the lower objective is updated as the new solution. An evolution based search method [10] utilized the history queries to approximate a Gaussian distribution as the search distribution. [6] formulated the decision-based attack problem as a continuous optimization by alternatively optimizing the perturbation magnitude and perturbation direction. This method was further accelerated in [7] by only estimating the sign of gradient. HopSkipJumpAttack [5] developed an iterative search algorithm by utilizing binary information at the decision boundary to estimate the gradient. It is further improved in [26] by learning a more representative subspace for perturbation sampling. Based on the observation of the low curvature of the decision boundary around adversarial examples, [29] approximated the gradient using the gradients of neighbour points; [35] locally approximated the decision boundary with a hyper-plane, and searched the closest point on the hyper-plane to the benign input as the perturbation.

**Score-based Adversarial Attacks.** There are generally three sub-categories of score-based black-box attacks, including *transfer-based* attack, *query-based attack* and their *combination*. **1) Transfer-based methods** attempt to generate adversarial perturbations utilizing the information of white-box surrogate models. For example, [33] proposed to firstly train a white-box surrogate model with a dataset labeled by querying the target model, then utilize the gradient of the trained surrogate model to generate adversarial perturbations to attack the target model. [28] found that adversarial perturbations generated on an ensemble of source models show good attack performance on the target model. Although transfer-based attack methods are very efficient, the attack performance is often lower than query-based attack methods. **2) Query-based methods** solve the black-box optimization by iteratively querying the target model. SimBA [14] randomly sampled a perturbation from a predefined orthonormal basis, and then either added or subtracted this perturbation to the attacked image. [22] utilized the natural evolution strategy (NES) [43, 44] method to minimize a continuous expectation of the black-box objective function based on a search distribution. Bandit [23] improved the NES method by incorporating data and temporal priors into the gradient estimation. SignHunter [1] adopted the

gradient sign rather than the gradient as the search direction. Query-based methods often achieve better attack performance than transfer-based methods, but require more queries. **3) Combination methods** try to take advantages of both transfer-based and query-based methods, to achieve high attack success rate and high query efficiency simultaneously. The general idea is firstly learning some types of priors from surrogate models, then incorporating these priors into the query-based method to guide the attack procedure for the target model. For example, the prior used in  $\mathcal{N}$ -Attack [27] is the mean parameter of the search distribution in NES, which is learned using a regression neural network trained based on surrogate models. Methods in [8] and [15] utilized the gradient of surrogate models as the gradient prior. The TREMBA method [21] treated the projection from a low-dimensional space to the original space as the prior, such that the perturbation could be search in the low-dimensional space. The hybrid method [41] directly adopted adversarial examples from surrogate models as the prior, but surrogate models could be updated using the returned prediction by the target model. The proposed method also belongs to this type, but the prior we adopted is the perturbation distribution.

### 3 Score-based Black-box Adversarial Attack

#### 3.1 Problem Formulation

We denote a classification model  $\mathcal{F} : \mathcal{X} \rightarrow \mathcal{Y}$ , with  $\mathcal{X}$  being the input space,  $n = |\mathcal{X}|$  indicating the dimension of the input space, and  $\mathcal{Y}$  being the output space, Given a benign example  $\mathbf{x} \in \mathcal{X}$  and its ground-truth label  $y \in \mathcal{Y}$ ,  $\mathcal{F}(\mathbf{x}, y)$  indicates the classification score w.r.t. the  $y$ -th label. In this work, we adopt the logit as the classification score. The goal of *adversarial attack* is finding a small perturbation  $\boldsymbol{\eta}$  within a  $\ell_p$ -ball, *i.e.*,  $\mathbb{B}_\epsilon = \{\boldsymbol{\eta} | \boldsymbol{\eta} \in \mathbb{R}^n, \|\boldsymbol{\eta}\|_p \leq \epsilon\}$  ( $\epsilon > 0$  being an attacker defined scalar, which will be specified in experiments), such that the prediction of  $\mathbf{x} + \boldsymbol{\eta}$  is different with the prediction of  $\mathbf{x}$ . Specifically, the *untargeted attack problem* is formulated as

$$\min_{\boldsymbol{\eta}} \mathcal{L}_{adv}^u(\boldsymbol{\eta}, \mathbf{x}, y) = \max \left( 0, \mathcal{F}(\mathbf{x} + \boldsymbol{\eta}, y) - \max_{j \neq y} \mathcal{F}(\mathbf{x} + \boldsymbol{\eta}, j) \right) + \delta(\boldsymbol{\eta} \in \mathbb{B}_\epsilon), \quad (1)$$

where  $\delta(a) = 0$  if  $a$  is true, otherwise  $\delta(a) = +\infty$ . The *targeted attack problem* is formulated as

$$\min_{\boldsymbol{\eta}} \mathcal{L}_{adv}^{tar}(\boldsymbol{\eta}, \mathbf{x}, t) = \max \left( 0, \max_{j \neq t} \mathcal{F}(\mathbf{x} + \boldsymbol{\eta}, j) - \mathcal{F}(\mathbf{x} + \boldsymbol{\eta}, t) \right) + \delta(\boldsymbol{\eta} \in \mathbb{B}_\epsilon). \quad (2)$$

Note that both  $\mathcal{L}_{adv}^u(\boldsymbol{\eta}, \mathbf{x}, y)$  and  $\mathcal{L}_{adv}^{tar}(\boldsymbol{\eta}, \mathbf{x}, t)$  are non-negative. If 0 is achieved, then the corresponding  $\boldsymbol{\eta}$  is a successful adversarial perturbation. For clarity, hereafter we use  $\mathcal{L}_{adv}(\boldsymbol{\eta}, \mathbf{x})$  to represent the untargeted or targeted attack when there is no need to distinguish between them.

In the case of *score-based black-box adversarial attacks*, the structure and parameters of the attacked model  $\mathcal{F}$  is inaccessible to the attacker, while only the output score  $\mathcal{F}(\mathbf{x}, y)$  is returned for each query  $\mathbf{x}$ . Consequently, the gradient of the attack objective  $\mathcal{L}_{adv}$  w.r.t. the perturbation  $\boldsymbol{\eta}$  cannot be directly computed, which is the main challenge of black-box adversarial attacks.

---

#### Algorithm 1 Evolution strategies for score-based black-box adversarial attacks

---

**input:** The black-box attack objective  $\mathcal{L}_{adv}(\cdot, \mathbf{x})$ , benign input  $\mathbf{x}$ , the ground-truth label  $y$  or the target label  $t$ , search distribution  $\pi$ , population size  $k$ .

**repeat**

(*Sampling*): sample  $k$  perturbations  $\boldsymbol{\eta}_1, \dots, \boldsymbol{\eta}_k \sim \pi$

(*Evaluation*): evaluate  $\mathcal{L}_{adv}(\boldsymbol{\eta}_1, \mathbf{x}), \dots, \mathcal{L}_{adv}(\boldsymbol{\eta}_k, \mathbf{x})$

(*Update*): update  $\pi$  to increase the probability of producing perturbations of potentially better objective values, *i.e.*, lower  $\mathcal{L}_{adv}(\cdot, \mathbf{x})$

**until** converge

---

#### 3.2 Evolutionary Strategies for Adversarial Attacks

One promising approach for the black-box optimization is evolutionary strategies (ES) [36]. The main idea is introducing a search distribution  $\pi$  to sample some perturbations  $\boldsymbol{\eta}$  to obtain the better values of the black-box objective function, *i.e.*, the smaller  $\mathcal{L}_{adv}$  in the score-based black-box adversarial attack problem. The general procedure of ES for the score-based black-box adversarial attack problem is summarized in Algorithm 1. Many variants of ES have been developed, such as natural ES (NES)

[43, 44], co-variance matrix adaptation ES (CMA-ES) [17], self-adaptation ES (SA-ES) [18, 38], *etc.* The main difference among these variants is the update step of the search distribution  $\pi$ . Among these variants, CMA-ES has been considered as one of the state-of-the-art variants in ES, especially for the optimization problem in high-dimensional space.

The basic idea of CMA-ES is to update the parameters of  $\pi$  by maximizing the weighted average of log-likelihoods  $\sum_{i=1}^m w_i \log \mathcal{P}_\pi(\boldsymbol{\eta}_{i:k})$ , where  $\log \mathcal{P}_\pi(\boldsymbol{\eta})$  denotes the log-likelihood of  $\boldsymbol{\eta}$  from the distribution  $\pi$ , where  $m, w_i, \boldsymbol{\eta}_{i:k}$  will be defined soon later. Consequently, it is more likely to sample perturbations of better values of the objective function, *i.e.*, lower values of  $\mathcal{L}_{adv}(\cdot, \mathbf{x})$ . The search distribution  $\pi$  used in CMA-ES is set to Gaussian, *i.e.*,  $\pi := \mathcal{N}(\boldsymbol{\mu}, \sigma^2 \cdot \mathbf{C})$ . Specifically, given the *Sampling* and *Evaluation* step in Algorithm 1, the *Update* step consists the following sequential parts:

- *Update  $\boldsymbol{\mu}$ :*

$$\boldsymbol{\mu}' = \boldsymbol{\mu}, \boldsymbol{\mu} \leftarrow \sum_{i=1}^m w_i \cdot \boldsymbol{\eta}_{i:k}, \quad (3)$$

where  $\boldsymbol{\eta}_{i:k}$  indicates the  $i$ -th best perturbation out of  $k$  sampled perturbations, *i.e.*,  $\mathcal{L}_{adv}(\boldsymbol{\eta}_{1:k}, \mathbf{x}) \leq \mathcal{L}_{adv}(\boldsymbol{\eta}_{2:k}, \mathbf{x}) \leq \dots \leq \mathcal{L}_{adv}(\boldsymbol{\eta}_{k:k}, \mathbf{x})$ , and  $m \leq k, \sum_{i=1}^m w_i = 1$  are hyper-parameters.

- *Update  $\sigma$ :*

$$\begin{cases} \mathbf{p}_\sigma \leftarrow (1 - c_\sigma)\mathbf{p}_\sigma + \sqrt{c_\sigma(2 - c_\sigma)\mu_{\text{eff}}} \mathbf{C}^{-\frac{1}{2}} \left( \frac{\boldsymbol{\mu} - \boldsymbol{\mu}'}{\sigma} \right), \\ \sigma \leftarrow \sigma \times \exp \left( \frac{c_\sigma}{d_\sigma} \left( \frac{\|\mathbf{p}_\sigma\|}{\mathbb{E}\|\mathcal{N}(\mathbf{0}, \mathbf{I})\|} - 1 \right) \right), \end{cases} \quad (4)$$

where  $\mathbb{E}\|\mathcal{N}(\mathbf{0}, \mathbf{I})\| = \sqrt{2}\Gamma(\frac{n+1}{2})/\Gamma(\frac{n}{2})$  with  $\Gamma(\cdot)$  being the gamma function [9].

- *Update  $\mathbf{C}$ :*

$$\begin{cases} \mathbf{p}_c \leftarrow (1 - c_\sigma)\mathbf{p}_c + h_\sigma \sqrt{c_c(2 - c_c)\mu_{\text{eff}}} \left( \frac{\boldsymbol{\mu} - \boldsymbol{\mu}'}{\sigma} \right), \\ \bar{w}_i = w_i \times (1 \text{ if } w_i \geq 0 \text{ else } k / \|\mathbf{C}^{-\frac{1}{2}} \left( \frac{\boldsymbol{\mu} - \boldsymbol{\mu}'}{\sigma} \right)\|^2), \\ \mathbf{C} \leftarrow \mathbf{C} + c_1 \mathbf{p}_c \mathbf{p}_c^\top + c_\mu \sum_{i=1}^m \bar{w}_i \left( \frac{\boldsymbol{\mu} - \boldsymbol{\mu}'}{\sigma} \right) \left( \frac{\boldsymbol{\mu} - \boldsymbol{\mu}'}{\sigma} \right)^\top. \end{cases} \quad (5)$$

We refer the readers to [17] for the detailed meanings of  $\mathbf{p}_\sigma, \mathbf{p}_c$ , as well as the empirical settings of all hyper-parameters ( $m, w_{i=1, \dots, m}, \mu_{\text{eff}}, d_\sigma, c_\sigma, c_\mu, c_c, c_1$ ). Furthermore, to reduce the number of parameters, we simply adopt the diagonal co-variance matrix  $\mathbf{C}$ , such that the search distribution can be represented as  $\pi := \mathcal{N}(\boldsymbol{\mu}, \text{diag}(\boldsymbol{\sigma}^2))$  with  $\boldsymbol{\sigma}^2 = [\sigma_1^2; \sigma_2^2; \dots; \sigma_n^2]$ .

## 4 Conditional Flow-based Models as the Search Distribution

### 4.1 Conditional Glow Model

In most variants of ES, a simple distribution is adopted as the search distribution, such as Gaussian distribution in CMA-ES. This simple setting has shown its effectiveness on solving many black-box optimization problems. However, it may be unsuitable for the black-box adversarial attack problem. Each adversarial perturbation is dependent on its corresponding benign example. Considering the diversity of benign examples, Gaussian distribution may not be capable and flexible enough to approximate the complex perturbation distributions conditioned on different benign examples.

**The c-Glow Model.** Inspired by the recent development in the literature of evolution strategies [12], we propose to replace the widely used Gaussian distribution by conditional generative flow models coupled with a Gaussian distribution as the search distribution  $\pi$ . Specifically, we adopt the one recently proposed model, dubbed the *conditional Glow* (c-Glow) model [30]. It can be formulated as an inverse function  $g_{\mathbf{x}, \phi} : \mathbf{z} \rightarrow \boldsymbol{\eta}$ , and there exists  $g_{\mathbf{x}, \phi}^{-1} : \boldsymbol{\eta} \rightarrow \mathbf{z}$ .  $\phi$  indicates the model parameter; the condition variable  $\mathbf{x}$  corresponds to the benign example;  $\mathbf{z} \in \mathbb{R}^{|\mathcal{X}|}$  is a latent variable following a simple distribution (specified later);  $\boldsymbol{\eta} \in \mathbb{R}^{|\mathcal{X}|}$  represents the perturbation variable. Further,  $g_{\phi, \mathbf{x}}$  can be decomposed to the composition of  $M$  inverse functions, as follows:

$$\boldsymbol{\eta} = g_{\mathbf{x}, \phi}(\mathbf{z}) = g_{\mathbf{x}, \phi_1}(g_{\mathbf{x}, \phi_2}(\dots(g_{\mathbf{x}, \phi_M}(\mathbf{z})))) \quad (6)$$

where  $\phi = (\phi_1, \dots, \phi_M)$ , and  $\phi_i$  indicates the parameter of  $g_{\mathbf{x}, \phi_i}(\cdot)$ . Note that each function can be implemented by a transformation layer. Then, the c-Glow model can be represented by a neural network with  $M$  layers, and we set  $M = 3$ . Each layer consists of a conditional actnorm module,

followed by an conditional  $1 \times 1$  convolutional module and a conditional coupling module. Due to the space limit, the detailed definition of  $g_{\mathbf{x}, \phi_i}(\cdot)$  will be presented in the **supplementary material**.

**Conditional Distribution with the c-Glow Model.** If  $\mathbf{z} = \boldsymbol{\mu} + \boldsymbol{\sigma} \odot \mathbf{z}_0$  with  $\mathbf{z}_0 \sim \mathcal{N}(\mathbf{0}, \mathbf{I})$ , where  $\odot$  is the entry-wise product and  $\mathbf{I}$  indicates the identity matrix, utilizing *the change of variables* [42] of Eq. (6), then the conditional likelihood of  $\boldsymbol{\eta}$  is formulated as

$$\log \mathcal{P}_{\boldsymbol{\theta}}(\boldsymbol{\eta}|\mathbf{x}) = \log \mathcal{P}_{\mathbf{0}, \mathbf{1}}(\mathbf{z}_0) + \sum_{i=1}^{M+1} \log \left| \det \left( \frac{\partial g_{\mathbf{x}, \phi_i}^{-1}(\mathbf{r}_{i-1})}{\partial \mathbf{r}_{i-1}} \right) \right|, \quad (7)$$

where  $\boldsymbol{\theta} = (\boldsymbol{\phi}, \boldsymbol{\mu}, \boldsymbol{\sigma})$ ,  $\mathbf{r}_i = g_{\phi_i, \mathbf{x}}^{-1}(\mathbf{r}_{i-1})$ ,  $\mathbf{r}_0 = \boldsymbol{\eta}$ ,  $\mathbf{r}_M = \mathbf{z}$  and  $\mathbf{r}_{M+1} = \mathbf{z}_0$ .  $\det(\cdot)$  indicates the determinant of a matrix.  $\mathcal{P}_{\mathbf{0}, \mathbf{1}}(\cdot)$  indicates the probability density function of the multi-variant normal distribution  $\mathcal{N}(\mathbf{0}, \mathbf{I})$ . Note that in the above equation, for simplicity, we treat the transformation  $\mathbf{z} = \boldsymbol{\mu} + \boldsymbol{\sigma} \odot \mathbf{z}_0$  as the  $M + 1$  layer of the c-Glow model, *i.e.*,  $g_{\mathbf{x}, \phi_{M+1}}(\mathbf{z}_0) = \boldsymbol{\mu} + \boldsymbol{\sigma} \odot \mathbf{z}_0$  with  $\phi_{M+1} = (\boldsymbol{\mu}, \boldsymbol{\sigma})$ , which is also invertible and independent with  $\mathbf{x}$ . Thus, we also have  $\boldsymbol{\eta} = g_{\mathbf{x}, \boldsymbol{\theta}}(\mathbf{z}_0)$ .

**Parameter Learning.** Consequently, we have  $\boldsymbol{\pi} := \mathcal{P}_{\boldsymbol{\theta}}(\boldsymbol{\eta}|\mathbf{x})$ . Compared to  $\mathcal{N}(\boldsymbol{\mu}, \text{diag}(\boldsymbol{\sigma}^2))$ , this new search distribution  $\mathcal{P}_{\boldsymbol{\theta}}(\boldsymbol{\eta}|\mathbf{x})$  is not only more capable to model the perturbation distribution due to the projection from the c-Glow model, but also more flexible for different benign examples due to its dependency on  $\mathbf{x}$ . However, in order to unleash these potential advantages, a good c-Glow model is required. Similar to [12], one feasible approach is to alternatively update  $(\boldsymbol{\mu}, \boldsymbol{\sigma})$  and  $\boldsymbol{\phi}$  when maximizing the weighted average of log-likelihoods in the update step of CMA-ES (see Section 3.2). However, it may require more queries to achieve good states of  $\boldsymbol{\phi}$ . Instead, we adopt a simple approach with two sequential steps, including: **1**) firstly pre-training the c-Glow model (including both  $(\boldsymbol{\mu}, \boldsymbol{\sigma})$  and  $\boldsymbol{\phi}$ ) in a different way (specified in the next sub-section); **2**) given the pre-trained mapping parameter  $\boldsymbol{\phi}$ , optimizing  $(\boldsymbol{\mu}, \boldsymbol{\sigma})$  using the standard CMA-ES algorithm (see Section 3.2).

## 4.2 Pre-training the c-Glow Model using Surrogate Models

### 4.2.1 Modeling the Perturbation Distribution via Energy-Based Models

Given a surrogate model  $\mathcal{F}_s : \mathcal{X} \rightarrow \mathcal{Y}$  with the same input and output space with the target model  $\mathcal{F}$ , we can adopt any off-the-shelf white-box adversarial attack method to generate adversarial perturbations. The adversarial loss of the untargeted attack is formulated as follows

$$\mathcal{L}_{adv, s}^u(\boldsymbol{\eta}, \mathbf{x}, y) = \max \left( \mathcal{F}_s(\mathbf{x} + \boldsymbol{\eta}, y) - \max_{j \neq y} \mathcal{F}_s(\mathbf{x} + \boldsymbol{\eta}, j) + \xi, 0 \right) + \delta(\boldsymbol{\eta} \in \mathbb{B}_\epsilon), \quad (8)$$

where the slack variable  $\xi \geq 0$  is introduced to enhance the flexibility (its value is specified in experiments), and  $\mathbb{B}_\epsilon$  has been defined in Eq. (1). Based on  $\mathcal{L}_{adv, s}^u(\boldsymbol{\eta}, \mathbf{x}, y)$ , we propose to utilize the energy based model to define the distribution of the untargeted adversarial perturbation  $\boldsymbol{\eta}$  around the benign example  $(\mathbf{x}, y)$ , as follows:

$$\mathcal{P}_s^u(\boldsymbol{\eta}|\mathbf{x}, y) = \frac{\exp(-\beta \cdot \mathcal{L}_{adv, s}^u(\boldsymbol{\eta}, \mathbf{x}, y))}{\int_{\boldsymbol{\eta} \in \mathbb{B}_\epsilon} \exp(-\beta \cdot \mathcal{L}_{adv, s}^u(\boldsymbol{\eta}, \mathbf{x}, y)) d\boldsymbol{\eta}}. \quad (9)$$

Note that given  $\mathcal{F}_s$ , the normalization term (*i.e.*, the denominator) is an intractable constant. Thus, we simply omit it hereafter, and set

$$\log \mathcal{P}_s^u(\boldsymbol{\eta}|\mathbf{x}, y) \approx -\lambda \cdot \mathcal{L}_{adv, s}^u(\boldsymbol{\eta}, \mathbf{x}, y), \quad (10)$$

where  $\beta, \lambda$  are two positive hyper-parameters. Later, we will use Eq. (10) to train the c-Glow model, and we only need to tune  $\lambda$  (see experiments). For the targeted attack of  $\mathcal{F}_s$ , the adversarial loss  $\mathcal{L}_{adv, s}^{tar}(\boldsymbol{\eta}, \mathbf{x}, t)$  ( $t$  is the target label), as well as the perturbation distribution  $\mathcal{P}_s^{tar}(\boldsymbol{\eta}|\mathbf{x}, t)$ , can be defined similarly. They are not presented here for clarity. Hereafter, we will use  $\mathcal{L}_{adv, s}(\boldsymbol{\eta}, \mathbf{x})$ ,  $\mathcal{P}_s(\boldsymbol{\eta}|\mathbf{x})$  to represent the adversarial loss and the perturbation distribution of  $\mathcal{F}_s$ , respectively, if there is no need to distinguish between untargeted and targeted attacks.

### 4.2.2 Training the c-Glow Model by Approximating the Perturbation Distribution

Recall the ES algorithm for adversarial attacks (see Algorithm 1), if the search distribution  $\mathcal{P}_{\boldsymbol{\theta}}(\boldsymbol{\eta}|\mathbf{x})$  (see Eq. (7)) is exactly the perturbation distribution of the attacked model  $\mathcal{F}$ , then the attack will be very efficient. However, in the scenario of black-box attacks, it is infeasible to explicitly model

the perturbation distribution of  $\mathcal{F}$  like that of  $\mathcal{F}_s$ , which requires a tremendous number of queries. Although the c-Glow model is capable to capture the perturbation distribution of  $\mathcal{F}$ , it may require lots of queries to achieve a good state of its parameters. Thus, we resort to the adversarial transferability [33, 28, 34] that the adversarial example generated for one model may be also adversarial for another model. Inspired by this observation, we assume that there is also somewhat similarity between the perturbation distributions of different models. Thus, we propose to pre-train the c-Glow model by minimizing the KL divergence [25] between  $\mathcal{P}_s(\boldsymbol{\eta}|\mathbf{x})$  and  $\mathcal{P}_\theta(\boldsymbol{\eta}|\mathbf{x})$ . Without loss of generality, here we only consider one benign example  $\mathbf{x}$ , then the training objective is formulated as

$$\min_{\boldsymbol{\theta}} \mathcal{L} = \mathbb{E}_{\mathcal{P}_s(\boldsymbol{\eta}|\mathbf{x})} \left[ \log \frac{\mathcal{P}_s(\boldsymbol{\eta}|\mathbf{x})}{\mathcal{P}_\theta(\boldsymbol{\eta}|\mathbf{x})} \right]. \quad (11)$$

We adopt the gradient-based method to optimize this problem. The gradient of  $\mathcal{L}$  w.r.t.  $\boldsymbol{\theta}$  is presented in Theorem 1. Due to the space limit, the proof of Theorem 1 will be presented in the **supplementary material**. Note that each term within the expectation in Eq. (12) is tractable, thus  $\nabla_{\boldsymbol{\theta}} \mathcal{L}$  can be easily computed. In practice,  $K$  instantiations of  $\mathbf{z}_0$  are sampled from  $\mathcal{N}(\mathbf{0}, \mathbf{I})$ , then  $\nabla_{\boldsymbol{\theta}} \mathcal{L}$  is empirically estimated as the average value over these  $K$  instantiations.  $K$  will be specified in experiments.

**Theorem 1.** Utilizing the definition  $\boldsymbol{\eta} = g_{\mathbf{x}, \boldsymbol{\theta}}(\mathbf{z}_0)$  and  $\mathbf{z}_0 \sim \mathcal{N}(\mathbf{0}, \mathbf{I})$  (see Section 4.1), and defining the term  $D(\boldsymbol{\eta}, \mathbf{x}) = \log \frac{\mathcal{P}_s(\boldsymbol{\eta}|\mathbf{x})}{\mathcal{P}_\theta(\boldsymbol{\eta}|\mathbf{x})}$ , then the gradient of  $\mathcal{L}$  w.r.t.  $\boldsymbol{\theta}$  is computed as follows

$$\begin{aligned} \nabla_{\boldsymbol{\theta}} \mathcal{L} &= -\mathbb{E}_{\mathbf{z}_0 \sim \mathcal{N}(\mathbf{0}, \mathbf{I})} \left[ \exp^{D(\boldsymbol{\eta}, \mathbf{x})} \cdot \nabla_{\boldsymbol{\eta}} D(\boldsymbol{\eta}, \mathbf{x})^\top \Big|_{\boldsymbol{\eta}=g_{\mathbf{x}, \boldsymbol{\theta}}(\mathbf{z}_0)} \cdot \nabla_{\boldsymbol{\theta}} g_{\mathbf{x}, \boldsymbol{\theta}}(\mathbf{z}_0) \right], \\ &= -\mathbb{E}_{\mathbf{z}_0 \sim \mathcal{N}(\mathbf{0}, \mathbf{I})} \left[ \frac{\exp^{-\lambda \cdot \mathcal{L}_{adv,s}(\boldsymbol{\eta}, \mathbf{x})}}{\mathcal{P}_\theta(\boldsymbol{\eta}|\mathbf{x})} \cdot \nabla_{\boldsymbol{\eta}} D(\boldsymbol{\eta}, \mathbf{x})^\top \Big|_{\boldsymbol{\eta}=g_{\mathbf{x}, \boldsymbol{\theta}}(\mathbf{z}_0)} \cdot \nabla_{\boldsymbol{\theta}} g_{\mathbf{x}, \boldsymbol{\theta}}(\mathbf{z}_0) \right], \end{aligned} \quad (12)$$

where  $\nabla_{\boldsymbol{\eta}} D(\boldsymbol{\eta}, \mathbf{x}) = \nabla_{\boldsymbol{\eta}} [-\lambda \cdot \mathcal{L}_{adv,s}(\boldsymbol{\eta}, \mathbf{x}) - \log \mathcal{P}_\theta(\boldsymbol{\eta}|\mathbf{x})]$ .

## 5 Experiments

### 5.1 Experimental Settings

**Datasets and Evaluation Metrics.** Following the setting in [11], we choose 1,000 images randomly from the testing set of CIFAR-10 [24] and the validation set of Tiny-ImageNet [37] for evaluation, respectively. For both datasets, we normalize the input to  $[0, 1]$  and set the maximum distortion of adversarial images to  $\epsilon = 8/255$ . The maximum number of queries is set to 10,000 for both untargeted and targeted attacks. As did in prior works [15, 31], we adopt the attack success rate (ASR), the mean and median number of queries of successful attacks to evaluate the attack performance.

**Target and Surrogate Models.** We consider four target models: VGG-15 [39], ResNet-Preact-110 [19], DenseNet-BC-110 [20] and PyramidNet-110 [16]. The implementations of these models are downloaded from a GitHub repository<sup>1</sup>. We conduct the standard training on the training set of each dataset to obtain the checkpoints of these target models. The top-1 error rates of these four target models are (7.29%, 6.47%, 4.69%, 3.92%) on the standard testing set of CIFAR-10, and (28.33%, 26.82%, 26.38%, 25.26%) on the standard validation set of Tiny-ImageNet, respectively. On each dataset, when attacking one target model, we treat the other three as surrogate models. For clarity, hereafter we use VGG, ResNet, DenseNet, PyramidNet to represent these target models.

**Compared methods.** Several state-of-the-art score-based black-box attack methods are compared, including Bandits [23], SimBA [14], Subspace [15], P-RGF [8], TREMBA [21], MetaAttack [11] and Signhunter [1]. All of them are implemented using the source codes provided by their authors.

**Implementation Details.** **1) Pre-training of the c-Glow model** is conducted on the standard training set of CIFAR-10 and Tiny-ImageNet, respectively. The adversarial loss  $\mathcal{L}_{adv,s}(\boldsymbol{\eta}, \mathbf{x})$  in Eq. (12) is specified as the average of CW-L2 losses [4] w.r.t. three surrogate models, and  $\xi$  is set as 20. We adopt the normalized gradient descent (NGD) [32] method to achieve the stable training. The batch-size is set as 2 and the learning rate is 0.0002. We sample  $K = 32$  instantiations of  $\mathbf{z}_0$  for each iteration of training. For finetuning the hyper-parameter  $\lambda$ , we randomly split 10% of the training set of CIFAR-10 and Tiny-ImageNet as validation set, and search  $\lambda$  within the range  $\{10, 20, \dots, 100\}$ . The fine-tuned values of  $\lambda$  are 20 for CIFAR-10 and 50 for Tiny-ImageNet. **2) The CMA-ES algorithm** is implemented using PyCMA<sup>2</sup>, with the population size  $k = 20$  and the selection size  $m = 10$ . The

<sup>1</sup>[https://github.com/hysts/pytorch\\_image\\_classification](https://github.com/hysts/pytorch_image_classification)

<sup>2</sup><https://github.com/CMA-ES/pycma>

Table 1: Attack success rate (ASR %), mean and median number of queries of untargeted attack and targeted attack (target class being 0) on CIFAR-10. The best and second-best values among methods that achieve more than 90% ASR are highlighted in bold and underline, respectively.

	Target Model → Attack Method ↓	ResNet			DenseNet			VGG			PyramidNet		
		ASR	Mean	Median	ASR	Mean	Median	ASR	Mean	Median	ASR	Mean	Median
Untargeted Attack	Bandits [23]	90.8	193.4	88.0	96.0	206.3	96.0	93.0	361.5	158.0	92.0	194.9	92.0
	SimBA [14]	<u>93.2</u>	432.1	235.0	74.0	480.5	223.0	68.3	632.3	237.0	84.0	455.5	270.0
	Subspace [15]	93.0	301.8	<u>12.0</u>	96.0	115.8	<u>12.0</u>	90.0	272.0	<u>12.0</u>	91.0	255.4	<u>10.0</u>
	P-RGF [8]	92.2	121.8	62.0	99.6	<u>111.7</u>	62.0	96.8	176.4	62.0	<u>98.2</u>	135.8	62.0
	TREMBA [21]	90.9	<u>120.7</u>	64.0	97.8	126.4	66.0	97.7	<u>125.5</u>	63.0	97.9	<u>82.3</u>	39.0
	MetaAttack [11]	<b>100.0</b>	363.2	153.0	<b>100.0</b>	411.5	225.0	<b>100.0</b>	392.0	161.0	<b>100.0</b>	320.4	191.0
	Signhunter [1]	<b>100.0</b>	135.1	47.0	<u>99.8</u>	213.8	119.0	93.3	244.3	102.0	97.5	161.9	69.0
	CG-ES (Ours)	<b>100.0</b>	<b>81.6</b>	<b>1.0</b>	<b>100.0</b>	<b>43.3</b>	<b>1.0</b>	<u>99.9</u>	<b>56.4</b>	<b>1.0</b>	<b>100.0</b>	<b>30.1</b>	<b>1.0</b>
	Targeted Attack	Bandits [23]	72.6	3660.1	2812.0	80.0	4154.8	3842.0	83.4	3967.6	3860.0	77.8	4484.6
SimBA [14]		<b>100.0</b>	940.0	885.0	<b>100.0</b>	838.8	777.0	<u>99.5</u>	1343.2	1210.0	<b>100.0</b>	<u>865.8</u>	779.0
Subspace [15]		78.0	2409.3	1630.0	94.0	1528.4	1012.0	67.0	2129.1	1366.0	80.0	2241.3	1586.0
P-RGF [8]		70.6	1020.8	390.0	77.1	1037.1	438.0	61.3	1083.9	360.0	50.3	1108.8	436.0
TREMBA [21]		91.2	1125.3	868.0	92.3	1123.4	879.0	96.5	<u>1331.5</u>	1142.0	98.1	1082.4	<u>759.0</u>
MetaAttack [11]		98.7	1953.3	1537.0	<u>99.8</u>	2013.7	1793.0	86.1	3045.6	2307.0	<u>98.9</u>	2054.6	1665.0
Signhunter [1]		<b>100.0</b>	<u>894.1</u>	<u>657.0</u>	<b>100.0</b>	<u>826.9</u>	<u>679.0</u>	<b>99.7</b>	1431.7	<u>1121.0</u>	<b>100.0</b>	1111.6	878.0
CG-ES (Ours)		<u>99.9</u>	<b>696.4</b>	<b>421.0</b>	<b>100.0</b>	<b>787.1</b>	<b>621.0</b>	98.8	<b>861.1</b>	<b>581.0</b>	<u>98.9</u>	<b>651.2</b>	<b>461.0</b>

mean  $\mu$  is initialized using the pre-trained c-Glow model, while the co-variance matrix  $\text{diag}(\sigma^2)$  is initialized as the identity matrix  $\mathbf{I}$ . All other hyper-parameters are set as default values in PyCMA.

## 5.2 Black-box Attack on CIFAR-10

**Untargeted Attack.** In this case, one attack is successful if the predicted class of the adversarial example is different from the ground-truth label. The results are reported in the top half of Table 1. It shows that the proposed CG-ES achieves 100% ASR on ResNet, DenseNet and PyramidNet, and 99.9% ASR on VGG, which demonstrates the effectiveness of our method. CG-ES is also very query-efficient. The mean number of queries is the lowest under all four target models in Table 1. More surprisingly, the median number of queries of CG-ES is just 1, which means that we successfully fool the target model with just one query for more than 50% attacked images. It reveals that the c-Glow model pre-trained on surrogate models is a good approximation to the perturbation distribution of the target model. In contrast, the second-best median queries are obtained by Subspace [15], which are more than 10x of ours, and with much lower ASR. The curves of the average ASR on all evaluation images v.s. the query number are shown in Fig. 1. It clearly highlights the superiority of our CG-ES method to all compared methods. Especially in the stage of low query numbers, CG-ES achieves very high ASR efficiently.

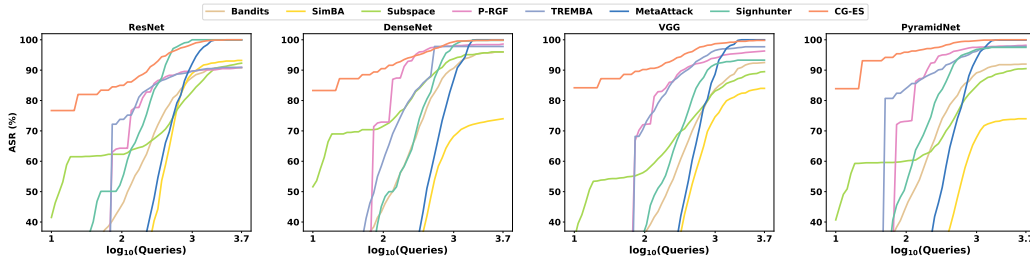


Figure 1: Attack success rate (ASR %) w.r.t. query numbers for untargeted attacks on CIFAR-10.

**Targeted Attack.** Following [21], we conduct targeted attacks with three target classes, including 0 (airplane), 4 (deer) and 9 (truck). When attacking for one target class, images with the same ground-truth class are skipped. Due to space limit, we report the attack results of the target class 0 in the bottom half of Table 1, and leave the results of the other two target classes in the **supplementary material**. As shown in Table 1, our CG-ES method achieves at least 98.8% ASR on all target models. Besides, the mean and median query numbers of CG-ES are significantly lower than that of all compared methods, demonstrating its query efficiency. Signhunter [1] obtains a slightly higher ASR than CG-ES on VGG (0.9% higher) and PyramidNet (1.1% higher), but with the cost of more than 1.6x query numbers.

Table 2: Attack success rate (ASR %), mean and median number of queries of untargeted attack and targeted attack (target class being 94) on Tiny-ImageNet. The best and second-best values among methods that achieve more than 90% ASR are highlighted in bold and underline, respectively.

	Target model → Attack Method ↓	ResNet			DenseNet			VGG			PyramidNet		
		ASR	Mean	Median	ASR	Mean	Median	ASR	Mean	Median	ASR	Mean	Median
Untargeted Attack	Bandits [23]	82.9	1846.6	168.0	77.6	2629.3	1194.0	81.8	2421.9	940.0	85.0	2508.1	1012.0
	SimBA [14]	<u>99.4</u>	616.9	398.0	<u>99.0</u>	1571.0	1198.0	97.5	1597.4	1168.0	97.5	1071.9	849.0
	Subspace [15]	78.6	642.0	6.0	86.9	778.4	10.0	81.4	975.9	10.0	83.3	856.7	10.0
	P-RGF [8]	98.2	203.2	112.0	91.2	<u>209.5</u>	112.0	91.8	452.0	<u>112.0</u>	95.3	482.9	112.0
	TREMBA [21]	99.1	139.3	<b>41.0</b>	98.1	221.2	<u>81.0</u>	98.8	<u>273.5</u>	<b>61.0</b>	99.0	211.3	<u>21.0</u>
	MetaAttack [11]	92.9	765.4	387.0	93.5	679.3	317.0	64.2	1352.5	1027.0	79.6	1015.7	642.0
	Signhunter [1]	<b>100.0</b>	<u>146.2</u>	<u>58.0</u>	<b>100.0</b>	383.5	156.0	<b>100.0</b>	316.4	113.0	<b>100.0</b>	<b>178.8</b>	68.0
	CG-ES (Ours)	<b>100.0</b>	<b>131.5</b>	<b>41.0</b>	98.9	<b>159.5</b>	<b>61.0</b>	<u>99.2</u>	<b>260.7</b>	<b>61.0</b>	99.4	<u>196.5</u>	<b>1.0</b>
Targeted Attack	Bandits [23]	47.4	5374.6	5592.0	41.7	6081.0	6476.0	44.2	5674.9	5910.0	47.8	4717.4	4582.0
	SimBA [14]	<b>100.0</b>	3407.1	3184.0	<b>92.9</b>	6061.8	5687.0	<b>91.6</b>	<b>6301.7</b>	<b>6020.0</b>	93.0	3816.2	3622.0
	Subspace [15]	47.0	5377.1	5256.0	42.0	3972.0	2268.0	41.2	5562.3	3982.0	47.8	4679.1	5412.0
	P-RGF [8]	54.6	3160.8	3286.0	59.4	3359.2	3187.0	52.1	3874.6	3429.0	55.3	3451.7	2466.0
	TREMBA [21]	74.3	3415.7	3014.0	81.2	3233.7	2972.0	77.3	3361.8	2978.0	73.2	3761.2	3320.0
	MetaAttack [11]	60.5	6332.2	6145.0	61.3	5863.8	5561.0	58.8	5979.4	5345.0	45.3	5995.2	5763.0
	Signhunter [1]	<b>100.0</b>	<u>2617.6</u>	<u>2239.0</u>	<u>92.6</u>	<u>3645.2</u>	<u>3123.0</u>	85.0	3123.1	2930.0	<u>95.9</u>	<u>2784.1</u>	<u>2078.0</u>
	CG-ES (Ours)	<b>100.0</b>	<b>2158.7</b>	<b>1761.0</b>	92.0	<b>3140.1</b>	<b>2801.0</b>	82.3	3315.1	3098.0	<b>96.0</b>	<b>2225.7</b>	<b>1581.0</b>

### 5.3 Black-box Attack on Tiny-ImageNet

**Untargeted Attack.** The results are summarized in the top half of Table 2. It shows that CG-ES performs better than compared methods at most cases. Specifically, when attacking the ResNet model, CG-ES achieves the highest ASR with the lowest mean and median number of queries among all methods. When attacking DenseNet, CG-ES achieves ASR of 98.9% with the lowest mean and median number of queries. The Signhunter is slightly higher than ours in terms of ASR (1.1% higher), but its mean and median number of queries are 2.4x of ours. In terms of VGG, CG-ES achieves the second-highest ASR and the best values of both mean and median number of queries. In terms of PyramidNet, CG-ES obtains the second-best values of both ASR and the mean number of queries, while the median query is just 1. In contrast, the median number of queries of Signhunter is 68x of ours. These comparisons demonstrate the effectiveness and efficiency of the proposed method.

**Targeted Attack.** Similar to that on CIFAR-10, we also randomly select three target classes: 94 (jellyfish), 113 (fly) and 171 (chain). Due to space limit, we report the results of the target class 94 in the bottom half of Table 2, and leave other results in the **supplementary material**. As shown in Table 2, our CG-ES is more effective and efficient than compared method at most cases. Specifically, when attacking ResNet and PyramidNet, CG-ES obtains the best performance on ASR, the mean and median number of queries. When attacking DenseNet, CG-ES also obtains the lowest mean and median number of queries. Although SimBA obtains slightly higher ASR (0.9% higher) than ours, its mean and median number of queries are about 1.9x of ours. For the target model VGG, CG-ES achieves the second-best value of mean number of queries. Above results demonstrate the superior performance of CG-ES.

### 5.4 Discussions

**Summary of Above Comparisons.** In all above results summarized in Tables 1-2, and there are 48 evaluation results in total. Among these results, our CG-ES method obtains 36 best and 6 second-best results. It fully demonstrates the superior performance of CG-ES on both effectiveness and efficiency, to all compared methods. Moreover, CG-ES always achieves the lowest median numbers of queries (except the targeted attack on VGG of Tiny-ImageNet), and even 1 at 4 results. It reflects that the search distribution  $\pi$  is very close to the intrinsic perturbation distribution of the target model, due to the powerful flexibility of the c-Glow model coupled with the Gaussian distribution, as well as the good transferability of the c-Glow model pre-trained on surrogate models.

**Supplementary Material.** Due to the space limit, some important information will be presented in the supplementary material, including: the detailed definition of the c-Glow model (see Section 4.1), the proof of Theorem 1, additional results of targeted attacks on both CIFAR-10 and Tiny-ImageNet, ablation studies about the effects of the c-Glow model and its initialization, as well as the empirical verification of the energy-based model for capturing the perturbation distribution (see Section 4.2.1).

**Future Extensions. 1)** The main idea of our method is replacing the search distribution in ES using the c-Glow model, while the ES algorithm is not influenced. Thus, our method is applicable to any ES variant, such as NES [43, 44]. **2)** As demonstrated in the last paragraph of Section 4.1, in this work we simply fix the parameter  $\phi$  of the c-Glow model as the pre-trained value, while only



fine-tuning the Gaussian parameters  $(\mu, \sigma)$ . Although this simple setting has shown surprisingly good performance, it is still interesting to explore what will happen if  $\phi$  is also fine-tuned. It is possible that the ASR could be further improved, as the search distribution  $\phi$  is supposed to be more close to the perturbation distribution of the target model. Above two extensions will be explored in our future work.

## 6 Conclusion

In this work, we proposed a novel search distribution in the evolution strategy (ES) method for solving the score-based black-box attack problem, based on the conditional Glow model coupled with the Gaussian distribution. This novel search distribution is flexible to capture the intrinsic distribution of adversarial perturbations conditioned on different benign examples. Besides, we proposed to pre-train the c-Glow model by approximating an energy-based model for the perturbation distribution of surrogate models. The pre-trained c-Glow model is then used as initialization in ES for attacking the target model. Consequently, the proposed CG-ES method takes advantages of both query-based and transfer-based attack methods, to obtain high attack success rate and high efficiency simultaneously. Extensive experiments of attacking four models on two benchmark datasets have fully verified the superior attack performance of the proposed method, compared to several state-of-the-art methods.

## References

- [1] Abdullah Al-Dujaili and Una-May O'Reilly. Sign bits are all you need for black-box attacks. In *ICLR*, 2020.
- [2] Battista Biggio, Igino Corona, Davide Maiorca, Blaine Nelson, Nedim Srndic, Pavel Laskov, Giorgio Giacinto, and Fabio Roli. Evasion attacks against machine learning at test time. In *ECML PKDD*, 2013.
- [3] Wieland Brendel, Jonas Rauber, and Matthias Bethge. Decision-based adversarial attacks: Reliable attacks against black-box machine learning models. In *ICLR*, 2018.
- [4] Nicholas Carlini and David A. Wagner. Towards evaluating the robustness of neural networks. In *IEEE S&P*, 2017.
- [5] Jianbo Chen, Michael I. Jordan, and Martin J. Wainwright. Hopskipjumpattack: A query-efficient decision-based attack. *arXiv preprint arXiv:1904.02144*, 2019.
- [6] Minhao Cheng, Thong Le, Pin-Yu Chen, Huan Zhang, Jinfeng Yi, and Cho-Jui Hsieh. Query-efficient hard-label black-box attack: An optimization-based approach. In *ICLR*, 2019.
- [7] Minhao Cheng, Simranjit Singh, Patrick H. Chen, Pin-Yu Chen, Sijia Liu, and Cho-Jui Hsieh. Sign-opt: A query-efficient hard-label adversarial attack. In *ICLR*, 2020.
- [8] Shuyu Cheng, Yinpeng Dong, Tianyu Pang, Hang Su, and Jun Zhu. Improving black-box adversarial attacks with a transfer-based prior. In *NeurIPS*, 2019.
- [9] Philip J. Davis. Leonhard euler's integral: A historical profile of the gamma function. *American Mathematical Monthly*, 66(10):849–869, 1959.
- [10] Yinpeng Dong, Hang Su, Baoyuan Wu, Zhifeng Li, Wei Liu, Tong Zhang, and Jun Zhu. Efficient decision-based black-box adversarial attacks on face recognition. In *CVPR*, 2019.
- [11] Jiawei Du, Hu Zhang, Joey Tianyi Zhou, Yi Yang, and Jiashi Feng. Query-efficient meta attack to deep neural networks. In *ICLR*, 2020.
- [12] Louis Faury, Clément Calauzènes, Olivier Fercoq, and Syrine Krichene. Improving evolutionary strategies with generative neural networks. *arXiv preprint arXiv:1901.11271*, 2019.
- [13] Ian J. Goodfellow, Jonathon Shlens, and Christian Szegedy. Explaining and harnessing adversarial examples. In *ICLR*, 2015.
- [14] Chuan Guo, Jacob R. Gardner, Yurong You, Andrew Gordon Wilson, and Kilian Q. Weinberger. Simple black-box adversarial attacks. In *ICML*, 2019.
- [15] Yiwen Guo, Ziang Yan, and Changshui Zhang. Subspace attack: Exploiting promising subspaces for query-efficient black-box attacks. In *NeurIPS*, 2019.

- [16] Dongyoon Han, Jiwhan Kim, and Junmo Kim. Deep pyramidal residual networks. In *CVPR*, 2017.
- [17] Nikolaus Hansen. The CMA evolution strategy: A tutorial. *arXiv preprint arXiv:1604.00772*, 2016.
- [18] Nikolaus Hansen, Dirk V. Arnold, and Anne Auger. Evolution strategies. In *Springer Handbook of Computational Intelligence*. 2015.
- [19] Kaiming He, Xiangyu Zhang, Shaoqing Ren, and Jian Sun. Identity mappings in deep residual networks. In *ECCV*, 2016.
- [20] Gao Huang, Zhuang Liu, Laurens van der Maaten, and Kilian Q. Weinberger. Densely connected convolutional networks. In *CVPR*, 2017.
- [21] Zhichao Huang and Tong Zhang. Black-box adversarial attack with transferable model-based embedding. In *ICLR*, 2020.
- [22] Andrew Ilyas, Logan Engstrom, Anish Athalye, and Jessy Lin. Black-box adversarial attacks with limited queries and information. In *ICML*, 2018.
- [23] Andrew Ilyas, Logan Engstrom, and Aleksander Madry. Prior convictions: Black-box adversarial attacks with bandits and priors. In *ICLR*, 2019.
- [24] Alex Krizhevsky, Geoffrey Hinton, et al. Learning multiple layers of features from tiny images. Technical report, Citeseer, 2009.
- [25] Solomon Kullback and Richard A Leibler. On information and sufficiency. *The Annals of Mathematical Statistics*, pages 79–86, 1951.
- [26] Huichen Li, Xiaojun Xu, Xiaolu Zhang, Shuang Yang, and Bo Li. QEBA: query-efficient boundary-based blackbox attack. In *CVPR*, 2020.
- [27] Yandong Li, Lijun Li, Liqiang Wang, Tong Zhang, and Boqing Gong. NATTACK: learning the distributions of adversarial examples for an improved black-box attack on deep neural networks. In *ICML*, 2019.
- [28] Yanpei Liu, Xinyun Chen, Chang Liu, and Dawn Song. Delving into transferable adversarial examples and black-box attacks. In *ICLR*, 2017.
- [29] Yujia Liu, Seyed-Mohsen Moosavi-Dezfooli, and Pascal Frossard. A geometry-inspired decision-based attack. In *ICCV*, 2019.
- [30] You Lu and Bert Huang. Structured output learning with conditional generative flows. In *AAAI*, 2020.
- [31] Seungyong Moon, Gaon An, and Hyun Oh Song. Parsimonious black-box adversarial attacks via efficient combinatorial optimization. In *ICML*, 2019.
- [32] Ryan Murray, Brian Swenson, and Soumya Kar. Revisiting normalized gradient descent: Fast evasion of saddle points. *IEEE Transactions on Automatic Control*, 64(11):4818–4824, 2019.
- [33] Nicolas Papernot, Patrick D. McDaniel, and Ian J. Goodfellow. Transferability in machine learning: from phenomena to black-box attacks using adversarial samples. *arXiv preprint arXiv:1605.07277*, 2016.
- [34] Nicolas Papernot, Patrick D. McDaniel, Ian J. Goodfellow, Somesh Jha, Z. Berkay Celik, and Ananthram Swami. Practical black-box attacks against machine learning. In *AISACCS*, 2017.
- [35] Ali Rahmati, Seyed-Mohsen Moosavi-Dezfooli, Pascal Frossard, and Huaiyu Dai. Geoda: a geometric framework for black-box adversarial attacks. In *CVPR*, 2020.
- [36] I Rechenberg. Evolutionsstrategien. In *Simulationmethoden in der Medizin und Biologie*. 1978.
- [37] Olga Russakovsky, Jia Deng, Hao Su, Jonathan Krause, Sanjeev Satheesh, Sean Ma, Zhiheng Huang, Andrej Karpathy, Aditya Khosla, Michael S. Bernstein, Alexander C. Berg, and Fei-Fei Li. Imagenet large scale visual recognition challenge. *International Journal of Computer Vision*, 115(3):211–252, 2015.

- [38] H.-P Schwefel. Numerische optimierung von computer-modellen mittels der evolutionsstrategie: mit einer vergleichenden einführung in die hill-climbing-und zufallsstrategie. In *Birkhäuser*, 1977.
- [39] Karen Simonyan and Andrew Zisserman. Very deep convolutional networks for large-scale image recognition. In *ICLR*, 2015.
- [40] Yi Sun, Daan Wierstra, Tom Schaul, and Jürgen Schmidhuber. Efficient natural evolution strategies. In *GECCO*, 2009.
- [41] Fnu Suya, Jianfeng Chi, David Evans, and Yuan Tian. Hybrid batch attacks: Finding black-box adversarial examples with limited queries. In *USENIX Security*, 2020.
- [42] Esteban G. Tabak and Eric Vanden-Eijnden. Density estimation by dual ascent of the log-likelihood. *Communications in Mathematical Sciences*, 8(1):217–233, 2010.
- [43] Daan Wierstra, Tom Schaul, Tobias Glasmachers, Yi Sun, Jan Peters, and Jürgen Schmidhuber. Natural evolution strategies. *The Journal of Machine Learning Research*, 15(1):949–980, 2014.
- [44] Daan Wierstra, Tom Schaul, Jan Peters, and Jürgen Schmidhuber. Natural evolution strategies. In *IEEE CEC*, 2008.